A numerical study of SSP time integration methods for hyperbolic conservation laws[*]

Nelida Črnjarić–Žic[1],[†], Bojan Crnković[1] and Senka Maćešić[1]

[1] *Faculty of Engineering, University of Rijeka, Vukovarska 58, HR-51 000 Rijeka, Croatia*

Abstract. The method of lines approach for solving hyperbolic conservation laws is based on the idea of splitting the discretization process in two stages. First, the spatial discretization is performed by leaving the system continuous in time. This approximation is usually developed in a non-oscillatory manner with a satisfactory spatial accuracy. The obtained semi-discrete system of ordinary differential equations (ODE) is then solved by using some standard time integration method.

In the last few years, a series of papers appeared, dealing with the high order strong stability preserving (SSP) time integration methods that maintain the total variation diminishing (TVD) property of the first order forward Euler method. In this work the optimal SSP Runge–Kutta methods of different order are considered in combination with the finite volume weighted essentially non-oscillatory (WENO) discretization. Furthermore, a new semi–implicit WENO scheme is presented and its properties in combination with different optimal implicit SSP Runge–Kutta methods are studied. Analysis is made on linear and nonlinear scalar equations and on Euler equations for gas dynamics.

AMS subject classifications: 65M06, 65M20, 35L65

Key words: WENO schemes, implicit schemes, hyperbolic conservation law, strong stability property, Runge–Kutta methods

1. Introduction

In this work we are interested in solving the one–dimensional hyperbolic conservation law system

$$\mathbf{u}_t + \mathbf{f}(\mathbf{u})_x = 0. \tag{1}$$

Here $\mathbf{u}$ denotes the state vector and $\mathbf{f}(\mathbf{u})$ denotes the flux. The commonly used method of lines approach [13] for solving this system results in a system of ordinary differential equations (ODE)

$$\frac{d\mathbf{u}}{dt} = \mathbf{L}(\mathbf{u}), \tag{2}$$

where $\mathbf{L}(\mathbf{u})$ denotes the approximation of the spatial derivative $-\mathbf{f}(\mathbf{u})_x$. The spatial approximation is usually obtained by using some nonlinear stable finite difference,

finite volume or finite element approximation. In this work, the finite volume WENO numerical schemes are used for the spatial discretization ([15, 10, 16, 9]).

Temporal discretization is done by using Runge-Kutta numerical methods for solving ODE. However, due to nonlinearity of the considered system and of spatial approximation, linearly stable methods could produce unsatisfactory numerical results [6, 5]. Moreover, when solving a hyperbolic system, numerical methods should approximate a discontinuous solution in a non oscillatory manner. The methods with the strong stability property have proven to be an appropriate choice for such problems. In this paper high-order strong stability preserving (SSP) time discretization methods for solving (2) are used. Due to their property of not increasing the total variation norm of the solution, these time discretization methods were first called TVD (total variation diminishing) methods (see [5]).

The key idea of the SSP methods is that strong stability achieved for the first order forward Euler method under a certain norm and for some time step restriction, is preserved for the higher order method under the same norm, perhaps under different time step restrictions. Therefore, if the nonlinear stability of spatial discretization coupled with the forward Euler time integration is achieved, the SSP time discretization maintains the stability property if the same spatial discretization is used with a higher order methods.

Recent development of SSP high order Runge-Kutta methods produced some interesting explicit and implicit methods for solving systems of ordinary differential equations. In [5, 7], a review of the explicit and implicit one-step and multistep SSP Runge-Kutta methods is given and their properties are studied. The explicit SSP Runge-Kutta methods, optimal in the sense that they admit the largest step size in the given class of methods, were developed in [6, 17]. Numerically optimal implicit SSP Runge-Kutta methods were developed in [11]. All optimal implicit methods determined in [11] actually belong to the class of diagonally implicit methods, and those of second and third order to the class of singly diagonally implicit. A detailed study of the strong stability preserving singly diagonally implicit (SDIRK) methods is done in [3], where the coefficients of these optimal methods are determined. An important result of the papers considering implicit SSP methods is that no unconditionally stable implicit SSP methods of order greater than one exist. Thus, all considered SSP methods have some time step stability barrier. In this work we use some explicit and SDIRK methods optimal in the sense that they use the maximal stepsize coefficient in the class of methods with the given order and number of stages. The coefficients for the optimal explicit Runge-Kutta methods are taken from [7] and for the optimal SDIRK methods from [3].

The time discretization process is described in Section 2 and some important results about the SSP Runge-Kutta discretization methods are briefly outlined. The spatial discretization performed by using the finite volume WENO discretization process is presented in Section 3. A combination of the considered WENO spatial discretization and the explicit SSP time integration method gives us the standard explicit finite volume WENO scheme ([15, 1]). On the other hand, if the implicit time discretization method is coupled with the finite volume WENO spatial approximation, the obtained fully implicit scheme could be computationally too expensive. By following the approach used in [19, 20], we propose to linearize the implicit terms

in an appropriate way. In this way, a new semi-implicit WENO scheme is obtained. A brief description of the proposed scheme is given in this paper. The presented numerical schemes are analyzed in Section 4 on linear and nonlinear scalar equations and on the Euler equations for gas dynamics. Stability properties of the explicit and semi-implicit WENO schemes coupled with the SSP time integration methods are studied.

2. SSP time integration methods

In this section, a brief overview of strong stability preserving Runge-Kutta one step methods that will be used in this paper is given.

As already mentioned in the introduction, the SSP time discretization methods were primarily developed for solving the hyperbolic conservation law systems (1). Thus, after the semi-discretization by the method of lines is applied, system (2) of ODE must be solved. Let us assume that the spatial operator $\mathbf{L}(\mathbf{u})$ arising in (2) has a property that in combination with the forward Euler time step

$$\mathbf{u}^{n+1} = \mathbf{u}^n + \Delta t \mathbf{L}(\mathbf{u}^n) \qquad (3)$$

becomes stable under certain norm and for a suitable time step restriction, i.e.,

$$||\mathbf{u}^{n+1}|| \leq ||\mathbf{u}^n||, \quad \text{for } \Delta t \leq \Delta t_{FE}.$$

The described property is referred to as a strong stability property, and the corresponding norms could be, for example, a total variation (TV) norm or an L_∞ norm.

The higher order SSP methods are obtained by requiring that the stability property achieved with the forward Euler time integration is preserved for the higher order method under eventually modified restrictions for the time step Δt. This restriction will be written in the form

$$\Delta t \leq c_{\text{SSP}} \Delta t_{\text{FE}},$$

where c_{SSP} denotes the SSP coefficient, defined as the largest coefficient for which the stability requirement is satisfied.

The necessity of the SSP property can be seen through some numerical results presented for example in [6, 5], which shows that if the linearly stable high-order methods are used in combination with a spatial discretization, the stability property could be lost, even if the method was a total variation diminishing in combination with the forward Euler method. Therefore, some other measure for the stability of numerical schemes was required. It appears that for solving hyperbolic problems, a strong stability property would be an appropriate choice [6, 17, 5, 7].

In this paper we use different higher order SSP Runge-Kutta time integration methods. A general s-stage Runge-Kutta method for solving system (2), written in

the Butcher form reads

$$\mathbf{u}^{(j)} = \mathbf{u}^n + \Delta t \sum_{l=1}^{s} \kappa_{lj} \mathbf{L}(\mathbf{u}^{(l)}), \quad j = 1, \ldots, s$$

$$\mathbf{u}^{n+1} = \mathbf{u}^n + \Delta t \sum_{l=1}^{s} b_l \mathbf{L}(\mathbf{u}^{(l)}). \tag{4}$$

The scheme is explicit if $\kappa_{lj} = 0$ for $l \geq j$, otherwise the scheme is implicit. Among all implicit schemes, we consider here the diagonally implicit schemes for which $\kappa_{lj} = 0$ for $l > j$, or more precisely, just singly diagonally implicit Runge-Kutta methods (SDIRK) for which, in addition, all the diagonal coefficients are equal. The order of the method depends on the coefficients κ_{jl} and b_l.

When considering the strong stability property of the explicit Runge-Kutta methods, a more convenient form of (4) would be the Shu-Osher formulation

$$\mathbf{u}^{(0)} = \mathbf{u}^n$$

$$\mathbf{u}^{(j)} = \sum_{l=0}^{j-1} \left(\alpha_{lj} \mathbf{u}^{(l)} + \Delta t \beta_{lj} \mathbf{L}(\mathbf{u}^{(l)}) \right), \quad j = 1, \ldots, s \tag{5}$$

$$\mathbf{u}^{n+1} = \mathbf{u}^{(s)}.$$

By consistency, the relation $\sum_{l=0}^{s} \alpha_{lj} = 1$, $j = 1, \ldots, s$ should be valid. It is known that for every Runge-Kutta method presented in Butcher form, there exists the corresponding Shu-Osher formulation, which is not unique. However, for every irreducible (see [3]) Runge-Kutta method, there exists its unique Butcher representation.

Besides the explicit methods, we are using optimal SDIRK methods developed in [3]. The methods are optimal in the sense that among all SDIRK methods with a given number of stages s and order of accuracy k, the value of the corresponding SSP coefficient is maximal, i.e., the largest time-step could be used. The coefficients κ_{lj} of Butcher formulation (4) and corresponding SSP coefficients of different optimal SDIRK methods for which the strong stability property holds can be found in [3].

There are some well known results for the SSP Runge-Kutta time discretization methods, which are briefly outlined in the proceeding.

1. If the forward Euler method (3) is strongly stable when solving system (2) under the restriction $\Delta t \leq \Delta t_{FE}$, then the explicit Runge-Kutta method (5) with $\alpha_{lj} \geq 0$ and $\beta_{lj} \geq 0$ is SSP, under the time step restriction

$$\Delta t \leq c(\alpha, \beta) \Delta t_{FE},$$

where $c(\alpha, \beta) = \min_{l,j} \frac{\alpha_{lj}}{\beta_{lj}}$. The maximal value of the coefficient $c(\alpha, \beta)$ over all Shu-Osher representations of the considered Runge-Kutta method is equal to the SSP coefficient c_{SSP}.

It is worth to note the difference between the CFL coefficient and the SSP coefficient. While the CFL coefficient prescribes a relation between the time step and the spatial step, the SSP coefficient prescribes the relation between the strong stability time step of a higher order scheme and the strong stability time step of the forward Euler method.

2. For $k = 2, 3$ the optimal explicit k-stage, kth-order SSP Runge-Kutta schemes with positive coefficients α_{lj} and β_{lj}, have the SSP coefficient equal to 1. The coefficients of these methods can be found, for example, in [5].

3. There exists no explicit 4-stage, 4th-order SSP Runge-Kutta scheme with positive coefficients β_{lj}, with the SSP coefficient > 0.
   There exists an explicit 5-stage, 4th-order SSP Runge-Kutta scheme with positive coefficients α_{lj}, β_{lj} with the SSP coefficient equal to 1.508. The method is developed in [17].

4. If the forward Euler method (3) is strongly stable when solving system (2) under some time step restriction, then the implicit backward Euler method is strongly stable without any time step restriction. Additionally, it was proved in [5] that the unconditionally stable implicit SSP Runge-Kutta method cannot have order higher than 1. However, there exist implicit SSP Runge-Kutta methods with finite SSP coefficients, i.e., $c_{\text{SSP}} < \infty$. A class of optimal implicit SSP Runge-Kutta methods is presented in [11].

5. The order of the s-stage SDIRK method cannot exceed $s + 1$. Furthermore, there exists no SSP SDIRK method of order greater than 4 (see [3]).

6. In [12] Kraaijevanger assigned the radius of absolute monotonicity $R(A, b)$ to each Runge-Kutta method written in the Butcher form. It was shown recently (see [7]) that for irreducible Runge-Kutta methods, this radius is equal to the optimal SSP coefficient. Since the value of $R(A, b)$ can be determined analytically, it becomes of great importance in the construction of higher order optimal SSP methods.

An interested reader is referred to [7, 5, 11, 4, 3] for more details about the SSP Runge-Kutta methods.

3. Finite volume WENO schemes

In order to solve the hyperbolic conservation law (1) with the finite volume WENO type scheme, the method of lines approach resulting in system (2) is used. In this section we describe more precisely the spatial discretization process, i.e., the process for determining the right-hand side of (2).

First, the spatial domain is divided into cells $I_i = [x_{i-\frac{1}{2}}, x_{i+\frac{1}{2}}]$, $i = 1, \ldots, N$ of the size Δx_i. It follows from (1) that the cell averages $\overline{\mathbf{u}}_i(t) = \frac{1}{\Delta x_i} \int_{x_{i-\frac{1}{2}}}^{x_{i+\frac{1}{2}}} \mathbf{u}(x, t) dx$ of the solution $\mathbf{u}(\cdot, t)$ over the cell I_i, satisfy an ordinary differential equation of the form

$$\frac{d\overline{\mathbf{u}}_i(t)}{dt} = -\frac{1}{\Delta x_i} \left(\mathbf{f}(\mathbf{u}(x_{i+\frac{1}{2}}, t)) - \mathbf{f}(\mathbf{u}(x_{i-\frac{1}{2}}, t)) \right), \quad i = 1, \ldots, N. \tag{6}$$

By replacing the terms on the right-hand side of (6) with their numerical approximations, the i-th equation of system (2) reads

$$\frac{d\overline{\mathbf{u}}_i(t)}{dt} = -\frac{1}{\Delta x_i} (\mathbf{f}_{i+\frac{1}{2}} - \mathbf{f}_{i-\frac{1}{2}}) \equiv \mathbf{L}_i(\overline{\mathbf{u}}). \tag{7}$$

For defining terms in (7), in this work we use the finite volume WENO discretization. For a detailed review of the standard WENO schemes we refer to papers [9, 16, 15]. A brief description of schemes follows.

The numerical flux $\mathbf{f}_{i+\frac{1}{2}}$ is evaluated by using an exact or approximate Riemann solver, i.e.,

$$\mathbf{f}_{i+\frac{1}{2}} = \mathbf{F}(\mathbf{u}_{i+\frac{1}{2}}^-, \mathbf{u}_{i+\frac{1}{2}}^+), \tag{8}$$

where $\mathbf{F}$ denotes the monotone numerical flux function, such as Roe flux, Godunov flux, etc. (see [13]). The values $\mathbf{u}_{i+\frac{1}{2}}^-$ and $\mathbf{u}_{i+\frac{1}{2}}^+$ are high order pointwise approximations to the solution $\mathbf{u}$ at the $(i + \frac{1}{2})$th cell boundary obtained from the known cell averages $\overline{\mathbf{u}}_i(t)$, $i = 1, \ldots, N$ by using the WENO reconstruction procedure.

In the proceeding, we first present an algorithm of the WENO reconstruction in the scalar case and then explain its enlargement to the vector case.

Let us consider the scalar function v. Suppose that the cell average values $\overline{v}_i$ of that function are known. The $(2r - 1)$th order WENO approximations $v_{i+\frac{1}{2}}^\pm$ on the $(i + 1/2)$th cell boundary can be computed as

$$v_{i+\frac{1}{2}}^\pm = \sum_{s=s_{min}^\pm}^{s_{max}^\pm} \sum_{k=0}^{r-1} \omega_{r,s}(\bar{v})^\pm a_{r,s,k}^\pm \overline{v}_{i-r+1+s+k}. \tag{9}$$

Here $s_{min}^- = 0$, $s_{max}^- = r - 1$, $s_{min}^+ = 1$ and $s_{max}^+ = r$. The coefficients $a_{r,s,k}^\pm$, $k = 0, \ldots, r - 1, s = s_{min}^\pm, \ldots, s_{max}^\pm$ depend on s, r, and cell sizes Δx_i, and not on the values $\overline{v}_i$. On the uniform mesh their values become independent of the cell sizes, and can be, for example, found in [15]. Furthermore, $\omega_{r,s}^\pm(\bar{v})$, $s = s_{min}^\pm, \ldots, s_{max}^\pm$ are the nonlinear weights, which depend on the local smoothness of the function v over the stencil $S_{r,s} = \{x_{i-r+1+s}, \ldots, x_{i+s}\}$, $s = s_{min}^\pm, \ldots, s_{max}^\pm$. In order to achieve the appropriate accuracy of the reconstruction, the nonlinear weights must satisfy some accuracy requirements [15]. They are typically evaluated in the following way

$$\omega_{r,s}(\bar{v}) = \frac{\alpha_{r,s}}{\sum_{j=0}^{r-1} \alpha_{r,j}}, \quad \alpha_{r,s} = \frac{C_{r,s}}{(\epsilon + IS_{r,s})^2}, \quad s = 0, \ldots, r - 1. \tag{10}$$

Here $C_{r,s}$ denote the ideal linear weights of the considered $(2r - 1)$th order WENO reconstruction belonging to the stencil $S_{r,s}$. The ideal linear weights for WENO reconstructions of different order can be found in [15]. Parameter ϵ is introduced to avoid that the denominator becomes zero and it is usually taken to be 10^{-6}. Coefficients $\omega_{r,s}(\bar{v})$ depend further on the smoothness indicators $IS_{r,s}$, which are some sort of the measure of smoothness of the interpolating polynomial p_i^s over the stencil $S_{r,s}$, which includes the cell I_i. They are usually evaluated as

$$IS_{r,s} = \sum_{l=1}^{r-1} \int_{I_i} \Delta x^{2l-1} \left(\frac{d^l p_i^s(x)}{dx^l} \right)^2 dx. \tag{11}$$

In the uniform mesh case the expressions for evaluating efficiently smoothness indicators that include the average function values with constant coefficients are known

(see [15]). With this we finish the description of the WENO reconstruction in the scalar case.

We describe now the WENO reconstruction in the vector case. There are two possible choices for the WENO reconstruction of the vector variable $\mathbf{u}$: the componentwise and the characteristicwise reconstruction. In the first case the described WENO reconstruction for the scalar function is performed for each component of the variable $\mathbf{u}$ separately. In the second case the vector variable is first transformed into local characteristic fields where the WENO reconstruction is made for each component and then the obtained values are transformed back into physical space. A detailed description of the WENO reconstruction with all needed coefficients can be found in [15].

We introduce here a common expression for both choices of WENO reconstructions of the state vector $\mathbf{u}$ in a vector form

$$\mathbf{u}^{\pm}_{i+\frac{1}{2}} = \sum_{s=s^{\pm}_{min}}^{s^{\pm}_{max}} \mathbf{\Omega}^{r,s,\pm}_{i+\frac{1}{2}}(\overline{\mathbf{u}}) \sum_{k=0}^{r-1} a^{\pm}_{r,s,k} \overline{\mathbf{u}}_{i-r+1+s+k}. \tag{12}$$

In the case of a componentwise WENO reconstruction the matrix $\mathbf{\Omega}^{r,s,\pm}_{i+\frac{1}{2}}(\overline{\mathbf{u}})$ is given with

$$\mathbf{\Omega}^{r,s,\pm}_{i+\frac{1}{2}}(\overline{\mathbf{u}}) = \mathrm{diag}[\omega^{\pm}_{r,s}(\bar{u}^1), \ldots, \omega^{\pm}_{r,s}(\bar{u}^m)],$$

where m denotes the number of equations of the considered conservation law and $\bar{u}^p$, $p = 1, \ldots, m$ stands for the p-th component of the state vector $\overline{\mathbf{u}}$.

In order to present a characteristicwise WENO reconstruction of the state vector $\mathbf{u}$, first the local characteristic fields must be defined. Let us take $\widehat{\mathbf{J}}_{f,i+\frac{1}{2}}$ to be a numerical approximation of the flux Jacobian $\mathbf{J}_f = \frac{d\mathbf{f}}{d\mathbf{u}}$ at $x_{i+\frac{1}{2}}$. We determine it as

$$\widehat{\mathbf{J}}_{f,i+\frac{1}{2}} = \mathbf{J}_f(\widehat{\mathbf{u}}_{i+\frac{1}{2}}),$$

where $\widehat{\mathbf{u}}_{i+\frac{1}{2}} = \mathbf{u}_{\mathrm{Roe}}(\mathbf{u}_i, \mathbf{u}_{i+1})$ denotes the Roe average of the states $\mathbf{u}_i$ and $\mathbf{u}_{i+1}$. Its value depends on the particular conservation law system. We denote with $\widehat{\mathbf{l}}^{(p)}_{i+\frac{1}{2}}$ and $\widehat{\mathbf{r}}^{(p)}_{i+\frac{1}{2}}$, $p = 1, \ldots, m$ left and right eigenvectors of the Jacobian matrix $\widehat{\mathbf{J}}_{f,i+\frac{1}{2}}$, respectively. For the characteristicwise WENO reconstruction of the state vector $\mathbf{u}$, the matrix $\mathbf{\Omega}^{r,s,\pm}_{i+\frac{1}{2}}(\overline{\mathbf{u}})$ in expression (12) reads

$$\mathbf{\Omega}^{r,s,\pm}_{i+\frac{1}{2}}(\overline{\mathbf{u}}) = \sum_{p=1}^{m} \omega^{\pm}_{r,s}(\overline{\mathbf{u}} \cdot \widehat{\mathbf{l}}^{(p)}_{i+\frac{1}{2}}) \left(\widehat{\mathbf{r}}^{(p)}_{i+\frac{1}{2}} \otimes \widehat{\mathbf{l}}^{(p)}_{i+\frac{1}{2}} \right),$$

where $\otimes$ denotes the tensor (diadic) product of vectors.

After the values $\mathbf{u}^{\pm}_{i+\frac{1}{2}}$ are determined, the approximate Riemann solver has to be applied. In this work the Roe solver given with

$$\mathbf{F}(\mathbf{u}^-_{i+\frac{1}{2}}, \mathbf{u}^+_{i+\frac{1}{2}}) = \frac{1}{2}(\mathbf{f}^-_{i+\frac{1}{2}} + \mathbf{f}^+_{i+\frac{1}{2}}) - \frac{1}{2}\mathbf{R}_{i+\frac{1}{2}}|\mathbf{\Lambda}_{i+\frac{1}{2}}|\mathbf{L}_{i+\frac{1}{2}}(\mathbf{u}^+_{i+\frac{1}{2}} - \mathbf{u}^-_{i+\frac{1}{2}}) \tag{13}$$

is used. Here $\mathbf{f}_{i+\frac{1}{2}}^{\pm} = \mathbf{f}(\mathbf{u}_{i+\frac{1}{2}}^{\pm})$. $\mathbf{L}_{i+\frac{1}{2}}$, $\mathbf{R}_{i+\frac{1}{2}}$, and $\mathbf{\Lambda}_{i+\frac{1}{2}}$ are matrices of left eigenvectors, right eigenvectors, and the diagonal matrix of the eigenvalues, respectively, belonging to a numerical approximation of the Jacobian matrix $\mathbf{J}_f(\widetilde{\mathbf{u}}_{i+\frac{1}{2}})$ at the Roe average $\widetilde{\mathbf{u}}_{i+\frac{1}{2}} = \mathbf{u}_{\mathrm{Roe}}(\mathbf{u}_{i+\frac{1}{2}}^{-}, \mathbf{u}_{i+\frac{1}{2}}^{+})$.

With this we conclude the definition of spatial discretization of the considered finite volume WENO scheme. At this point the system of ordinary differential equations (2) must be solved by using the presented explicit or implicit SSP Runge-Kutta method.

If the explicit Runge-Kutta time integration is used, the numerical solution can be simply evaluated. On the other hand, if the implicit time integration is used, a non-linear system of equations is obtained. For determining its solution some standard numerical procedures such as Newton iterations can be applied. However, such a scheme could become computationally too expensive. Therefore in this work we use a semi-implicit WENO scheme. This scheme is based on the appropriate linearization of the implicit WENO numerical scheme by following the approach used in [2, 19, 20]. We describe the linearization process and the obtained semi-implicit scheme in more details. Let us suppose that the SDIRK method of the form (4) is used. In order to linearize each step of the Runge-Kutta method, vector $\mathbf{f}_{i+\frac{1}{2}}^{(j),\pm}$ that appears in terms $\mathbf{L}_i(\mathbf{u}^{(j)})$, $i = 1, \ldots, N$ after introducing the numerical flux (13), is linearized by using a local Taylor expansion

$$\mathbf{f}_{i+\frac{1}{2}}^{(j),\pm} \approx \mathbf{f}_{i+\frac{1}{2}}^{(j-1),\pm} + \mathbf{J}_{f,i+\frac{1}{2}}^{(j-1),\pm}\left(\mathbf{u}_{i+\frac{1}{2}}^{(j),\pm} - \mathbf{u}_{i+\frac{1}{2}}^{(j-1),\pm}\right), \tag{14}$$

around the states $\mathbf{u}_{i+\frac{1}{2}}^{(j-1),\pm}$ from the preceding iteration level. Here

$$\mathbf{J}_{f,i+\frac{1}{2}}^{(j-1),\pm} = \mathbf{J}_f(\mathbf{u}_{i+\frac{1}{2}}^{(j-1),\pm}).$$

Notice that $\mathbf{L}_i(\mathbf{u}^{(j)})$, $i = 1, \ldots, N$ are the building blocks of the term $\mathbf{L}(\mathbf{u}^{(j)})$, which arises in the Runge-Kutta method. Furthermore, we suppose that when evaluating the numerical flux (13), the characteristic decomposition, i.e., matrices of left and right eigenvectors and the matrix of eigenvalues are taken from the preceding and not the current iteration level. By introducing these approximations into the spatial discretization (7), it follows

$$\mathbf{L}_i(\mathbf{u}^{(j)}) \approx \mathbf{L}_i(\mathbf{u}^{(j-1)}) - \frac{1}{\Delta x_i}\left(\mathbf{F}_{i+\frac{1}{2}}^{-}(\mathbf{u}_{i+\frac{1}{2}}^{(j),-} - \mathbf{u}_{i+\frac{1}{2}}^{(j-1),-}) + \mathbf{F}_{i+\frac{1}{2}}^{+}(\mathbf{u}_{i+\frac{1}{2}}^{(j),+} - \mathbf{u}_{i+\frac{1}{2}}^{(j-1),+})\right.$$
$$\left. -\mathbf{F}_{i-\frac{1}{2}}^{-}(\mathbf{u}_{i-\frac{1}{2}}^{(j),-} - \mathbf{u}_{i-\frac{1}{2}}^{(j-1),-}) - \mathbf{F}_{i-\frac{1}{2}}^{+}(\mathbf{u}_{i-\frac{1}{2}}^{(j),+} - \mathbf{u}_{i-\frac{1}{2}}^{(j-1),+}),\right) \tag{15}$$

where the terms

$$\mathbf{F}_{i+1/2}^{\pm} = \frac{1}{2}\left(\mathbf{J}_{f,i+1/2}^{\pm} \mp \mathbf{R}_{i+\frac{1}{2}}|\mathbf{\Lambda}_{i+\frac{1}{2}}|\mathbf{L}_{i+\frac{1}{2}}\right) \tag{16}$$

are evaluated at the preceding iteration level.

At this moment, we additionally suppose that the non-linear weights of the WENO reconstruction for the solution $\mathbf{u}^{(j-1)}$ on the preceding iteration level and

for the solution $\mathbf{u}^{(j)}$ on the current iteration level are equal. It is worth to note that the order of accuracy is not lost with the introduced approximation, since for smooth solutions the WENO non-linear weights are equal to the ideal linear weights for which $(2r-1)$-th order reconstruction is attained and they do not depend on the function reconstruction values. By introducing the approximation (15) and the expression (12) for the WENO reconstructions of terms $\mathbf{u}_{i\pm\frac{1}{2}}^{(j-1),\pm}$ and $\mathbf{u}_{i\pm\frac{1}{2}}^{(j),\pm}$, the numerical step (4) of the SDIRK Runge-Kutta scheme can be written in the form

$$\mathbf{u}^{(j)} = \mathbf{u}^{(0)} + \Delta t \sum_{l=1}^{j-1} \kappa_{lj}\mathbf{L}(\mathbf{u}^{(l)}) + \Delta t \kappa_{jj}\mathbf{L}(\mathbf{u}^{(j-1)})$$

$$+\Delta t \kappa_{jj}\mathbf{K}(\mathbf{u}^{(j-1)})(\mathbf{u}^{(j)} - \mathbf{u}^{(j-1)}), \quad j = 1, \ldots, s. \quad (17)$$

The matrix $\mathbf{K}(\mathbf{u}^{(j-1)})$ is a block $(2r+1)$-diagonal matrix of dimension $mN \times mN$. Its building blocks are $m \times m$ matrices of the form

$$\mathbf{K}_{i,i-r+1+k} = -\frac{1}{\Delta x_i} \sum_{s=0}^{r} \left(a_{r,s,k-s}^{-} \mathbf{F}_{i+\frac{1}{2}}^{-} \mathbf{\Omega}_{i+\frac{1}{2}}^{r,s,-} + a_{r,s,k-s}^{+} \mathbf{F}_{i+\frac{1}{2}}^{+} \mathbf{\Omega}_{i+\frac{1}{2}}^{r,s,+} \right.$$

$$\left. - a_{r,s,k-s+1}^{-} \mathbf{F}_{i-\frac{1}{2}}^{-} \mathbf{\Omega}_{i-\frac{1}{2}}^{r,s,-} - a_{r,s,k-s+1}^{+} \mathbf{F}_{i-\frac{1}{2}}^{+} \mathbf{\Omega}_{i-\frac{1}{2}}^{r,s,+} \right), \quad (18)$$

$k = 0, \ldots, 2r$, $i = 1, \ldots, N$. The terms of these matrices are derived by using expressions (15) and (12). Since we express matrices $\mathbf{K}_{i,i-r+1+k}$ in the compact form (18), there could arise combinations of indexes s and k in the above sum for which the coefficients $a_{r,s,k}^{\pm}$ are not defined with the WENO reconstruction procedure. In these cases we simply suppose that these coefficients are equal to 0.

It follows from (17) that at each time step the linear system of the form

$$(\mathbf{I} - \Delta t \kappa_{jj}\mathbf{K}(\mathbf{u}^{(j-1)}))\Delta\mathbf{u}^{(j)} = RHS, \quad j = 1, \ldots, s, \quad (19)$$

with unknowns $\Delta\mathbf{u}^{(j)} = \mathbf{u}^{(j)} - \mathbf{u}^{(j-1)}$ and the right-hand side equal to

$$RHS = -\sum_{l=1}^{j-1} \Delta\mathbf{u}^{(l)} + \Delta t \sum_{l=1}^{j-1} \kappa_{lj}\mathbf{L}(\mathbf{u}^{(l)}) + \Delta t \kappa_{jj}\mathbf{L}(\mathbf{u}^{(j-1)}) \quad (20)$$

must be solved. One can note that at each step all terms in (20) are known from previous stages of the used SDIRK scheme. For small enough time step Δt, the matrix of the system (19) is regular and the solution of the system is unique.

We conclude this section with a brief algorithm of the finite volume WENO scheme, which is applied for each time step and at each stage of the used Runge-Kutta method (4):

- Determine the $(2r-1)$th order approximations $\mathbf{u}_{i+\frac{1}{2}}^{(j-1),-}$ and $\mathbf{u}_{i+\frac{1}{2}}^{(j-1),+}$ by using (12) and the values $\mathbf{u}^{(j-1)}$ for all $i = 1, \ldots, N$.

- If the explicit scheme is used, determine spatial approximations $\mathbf{L}_i(\mathbf{u}^{(j-1)})$, $i = 1, \ldots, N$ and use them for evaluating the states $\mathbf{u}^{(j)}$ on the new iteration level by applying the appropriate stage of the Runge-Kutta time integration.

• If the implicit scheme is used, determine spatial approximations $\mathbf{L}_i(\mathbf{u}^{(j-1)})$, $i = 1, \ldots, N$ and the matrix $\mathbf{K}(\mathbf{u}^{(j-1)})$ arising in (17), by using the weights of the WENO reconstruction and other terms from the preceding iteration level. Compute expression (20) and solve system (19) to obtain new states $\mathbf{u}^{(j)}$.

4. Numerical tests

In this section we present numerical results obtained on the linear and non-linear scalar equations and on the Euler equations for gas dynamics. In the considered tests we have mainly focused on the SSP property of the presented numerical schemes with the explicit and semi-implicit finite volume discretizations. Furthermore, we compare the behaviour of the explicit and semi-implicit WENO schemes coupled with the SSP time integration methods.

The following notation is used. With SSPERK WENO (s, k, r) we denote the schemes constructed by the SSP explicit Runge-Kutta time integration of k-th order and with s stages, and space discretization with $(2r - 1)$-th order WENO reconstruction. Similarly, the notation SDIRK WENO (s, k, r) is used for semi-implicit schemes with the SDIRK time integration methods and with an appropriate number of stages and order.

4.1. Linear advection

Several numerical tests were performed on the linear advection equation

$$u_t + u_x = 0. \tag{21}$$

4.1.1. Test for the stability with simple shock

The stability property of different numerical schemes is investigated on the test problem with the initial condition

$$u(x, 0) = \begin{cases} 1, & x < 1 \\ 0, & x > 1 \end{cases}$$

on the domain $[0, 2]$.

Stability analysis of numerical schemes is performed in the following way. First, stability properties of the finite volume WENO spatial discretizations of different orders coupled with the first order forward Euler time integration are considered. More precisely, we determine maximal time steps for which the total variation of the solution does not increase for more than ϵ. The obtained time steps are denoted with Δt_{FE} and the corresponding CFL coefficients with $c_{\text{TVD}}(1, 1, r) = \Delta t_{\text{FE}}/\Delta x$. Here r stands for the parameter of the corresponding WENO reconstruction of order $2r - 1$. In all performed computations we use the space step $\Delta x = 0.01$. The stability barrier is chosen to be $\epsilon = 10^{-3}$. This critical value was determined experimentally, based on a large number of numerical computations, as a value for which a clear distinction between the round-off errors and numerical oscillations can be made.

The following practical CFL coefficients are obtained:

$$c_{\text{TVD}}(1, 1, 3) = 0.5, \quad c_{\text{TVD}}(1, 1, 4) = 0.42, \quad c_{\text{TVD}}(1, 1, 5) = 0.36.$$

The described procedure is then performed for the finite volume WENO explicit and semi-implicit numerical schemes with different spatial and SSP time discretizations. With $c_{\text{TVD}}(s, k, r)$ we denote the maximal CFL coefficient for which the TV norm of the solution obtained with the numerical scheme composed by the k-th order SSP Runge-Kutta time integration with s stages and with $(2r - 1)$-th order WENO spatial discretization does not increase for more than ϵ. In Figure 1 we present some typical instabilities that occur when the time step larger than a critical time step determined by the coefficient $c_{\text{TVD}}(s, k, r)$ is used. Furthermore, changes in total variation of the solution for the chosen numerical scheme are presented.
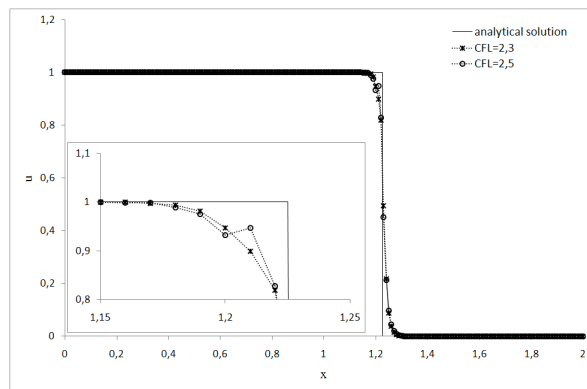
(a) *Numerical solutions at $t = 0.225s$*
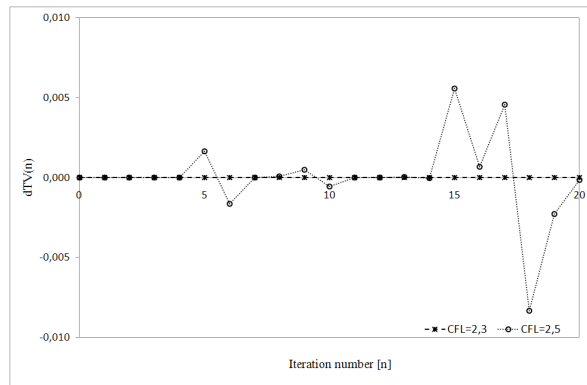
(b) *Difference in TV norm of the solutions, $dTV(n) = TV(u^n) - TV(u^{n-1})$*

Figure 1. *TEST 4.1.1 – Typical instabilities of numerical results and difference in TV norm of solution obtained with SDIRK WENO (3,3,4) scheme by using stable and non-stable time step*

Num. scheme	$c_{\mathrm{TVD}}(s,k,r)$	$\sigma_{\mathrm{SSP}}(s,k,r)$	c_{SSP}	c_{eff}
SSPERK WENO (2,2,3)	0.75	1.50	1.00	0.38
SSPERK WENO (3,3,4)	0.65	1.55	1.00	0.22
SSPERK WENO (5,4,5)	1.00	2.78	1.51	0.20
SDIRK WENO (1,2,3)	0.95	1.90	2.00	0.95
SDIRK WENO (2,2,3)	1.30	2.60	4.00	0.65
SDIRK WENO (3,2,3)	2.40	4.80	6.00	0.80
SDIRK WENO (2,3,4)	1.30	3.10	2.73	0.65
SDIRK WENO (3,3,4)	2.30	5.48	4.83	0.77
SDIRK WENO (4,3,4)	3.10	7.38	6.87	0.78
SDIRK WENO (5,3,4)	3.70	8.81	8.90	0.74
SDIRK WENO (3,4,5)	1.40	3.89	1.76	0.47
SDIRK WENO (4,4,5)	1.80	5.00	4.21	0.45
SDIRK WENO (5,4,5)	2.30	6.39	5.74	0.46
SDIRK WENO (6,4,5)	2.80	7.78	7.55	0.47
SDIRK WENO (7,4,5)	3.50	9.72	8.67	0.50
SDIRK WENO (8,4,5)	3.50	9.72	10.23	0.44

Table 1. *Test 4.1.1 – Stability coefficients for different explicit and semi-implicit numerical schemes with finite volume WENO space discretizations*

Finally, for each considered scheme we determine the practical SSP coefficient $\sigma_{\mathrm{SSP}}(s,k,r)$ as

$$\sigma_{\mathrm{SSP}}(s,k,r) = \frac{c_{\mathrm{TVD}}(s,k,r)}{c_{\mathrm{TVD}}(1,1,r)}.$$

The idea is to compare those values with theoretical SSP coefficients c_{SSP} of the considered schemes. Schemes coefficients and theoretical SSP coefficients can be found in [11, 3]. The values obtained experimentally for different numerical schemes are presented in Table 1.

For all tested numerical schemes with the exception of schemes with the second order SDIRK time integration and fourth order SDIRK with 8 stages, the determined practical SSP coefficients $\sigma_{\mathrm{SSP}}(s,k,r)$ are greater than the theoretically established c_{SSP}. We have to mention that the WENO space discretization is not proved to be TVD, thus the necessary conditions which guarantee the SSP property of the scheme are not theoretically fulfilled. However, despite the lack of theoretical results, practical computations show that the SSP property is actually satisfied.

In order to measure and compare relative efficiency of the considered schemes in Table 1 we furthermore present effective CFL coefficients c_{eff} obtained by dividing $c_{\mathrm{TVD}}(s,k,r)$ by the number of stages s required for each method. One can observe that for semi-implicit schemes with the second order time integration methods these coefficient are variable (between 0.65 and 0.95), while for the third and fourth order time integrations they are quite unified. For the third order schemes they lie between 0.65 and 0.75 and for the fourth order schemes between 0.44 and 0.5. For explicit numerical schemes these effective coefficients are much smaller than for the semi–implicit ones.
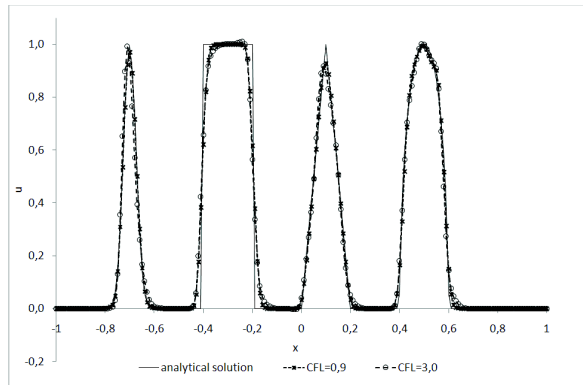
4.1.2. Linear advection test
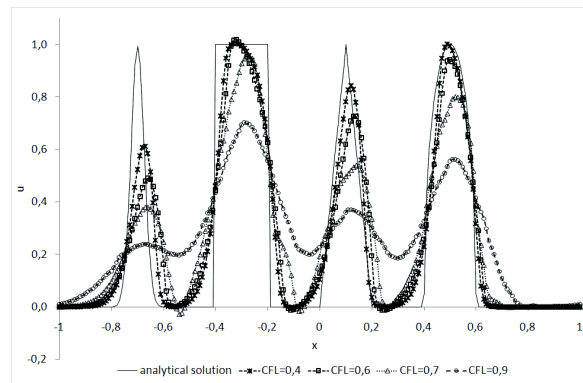
(a) *SSPERK WENO (2,2,3)*
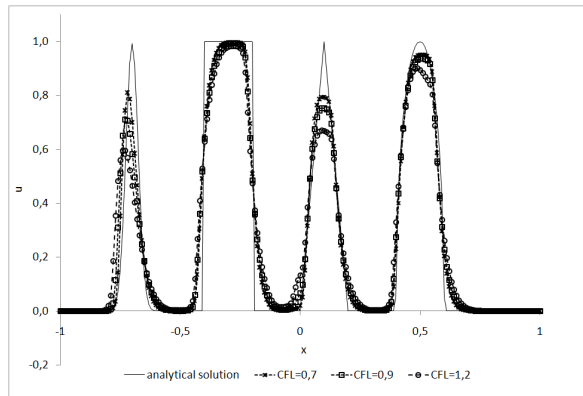
(b) *SDIRK WENO (2,3,4)*

(c) *SDIRK WENO (7,4,5)*

Figure 2. *TEST 4.1.2 – Comparison of numerical results obtained for different time steps at t = 8s*

We furthermore analyze the behaviour of schemes with different SSP time integration methods on the test problem that was suggested in [10], with initial condition

$$u(x,0) = \begin{cases} \frac{1}{6}\left[G(x, z-\delta) + 4G(x,z) + G(x, z+\delta)\right], & -0.8 \le x \le -0.6 \\ 1, & -0.4 \le x \le -0.2 \\ 1 - |10(x-0.1)|, & 0 \le x \le 0.2 \\ \frac{1}{6}\left[F(x, a-\delta) + 4F(x,a) + F(x, a+\delta)\right], & 0.4 \le x \le 0.6 \\ 0, & \text{otherwise} \end{cases},$$

where $G(x,z) = e^{-\beta(x-z)^2}$, $F(x,a) = \sqrt{\max(1 - \alpha^2(x-a)^2, 0)}$ and constants equal to $a = 0.5$, $z = -0.7$, $\delta = 0.005$, $\alpha = 10$, and $\beta = \frac{\log 2}{36\delta^2}$. The boundary conditions are defined as periodic on the domain $[-1, 1]$. We compute the solution up to $t = 8s$ and with $\Delta x = 0.01$.

In Figure 2 we present the behaviour of finite volume WENO schemes with SSP explicit and SDIRK time integration methods at $t = 8s$. There are few things that can be noticed. First, numerical schemes which use the second order time integration produce quite diffusive numerical results. In all the presented figures, instabilities that occur for the time steps greater than critical time steps achieved in Test 1 are visible. On the other hand, if the time step is bounded by the determined SSP values, stable results are obtained. Moreover, numerical results obtained with explicit and semi-implicit schemes with the same time step restriction CFL=0.7 are compared in Figure 3. One can see that a lower numerical diffusion and a better coincidence with the analytical solution can be observed on the first three waves for semi-implicit schemes, while numerical results obtained by using the explicit scheme coincide better with the analytical solution on the last smoother wave.
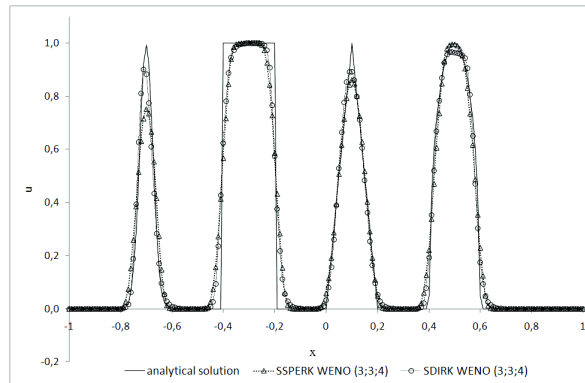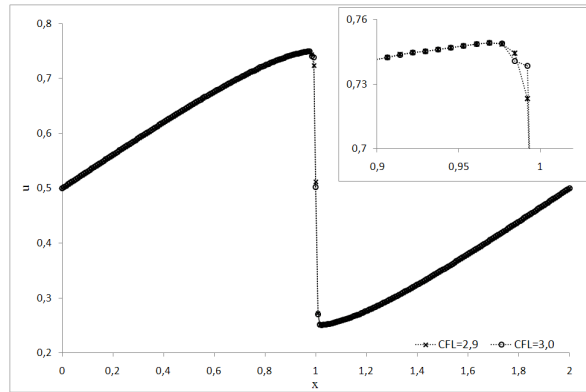

Figure 3. *TEST 4.1.2 – Comparison of numerical results obtained with explicit and semi-implicit numerical schemes of equal order and step size with CFL=0.7, $t = 8s$*
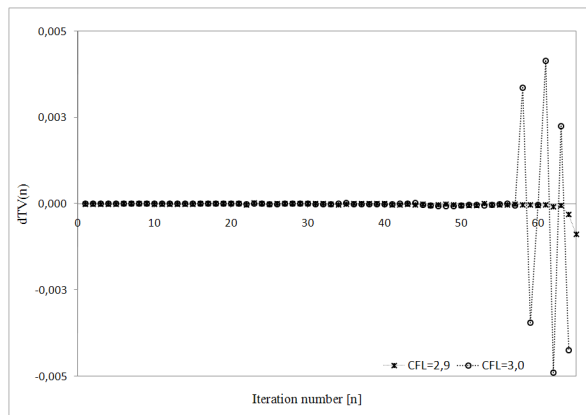
4.2. Burger's equation

We consider a non-linear scalar Burger's equation

$$u_t + \left(\frac{1}{2}u^2\right)_x = 0, \tag{22}$$

(a) *Numerical solutions at* $t = 2s$

(b) *Difference in TV norm of solutions,* $dTV(n) = TV(u^n) - TV(u^{n-1})$

Figure 4. *TEST 4.2 – Comparison of numerical results and difference in TV norms of solutions obtained with SDIRK WENO (4,3,4) by using stable and non-stable time step*

with the initial condition $u(x,0) = 0.5 - 0.25\sin(\pi x)$ and periodic boundary conditions on the domain $[0,2]$. The practical region of stability for different numerical schemes is analyzed. Practical coefficients $c_{\mathrm{TVD}}(s,k,r)$ are determined in the same way as for the linear advection test 4.1.1, i.e., $c_{\mathrm{TVD}}(s,k,r)$ is the largest coefficient for which the total variation norm of the solution between two states does not increase for more than 10^{-3}. In order to analyze the appearance of numerical instabilities, numerical computations were performed for different computational times. From this we have concluded that, after the shock in solution forms, the TV seminorm of the solution decreases rapidly and numerical schemes become more stable. Therefore, the results are studied up to the final time $t = 2s$, when the shock in the solution forms and larger instabilities occur.

In Figure 4, typical instabilities that occur for the CFL coefficients greater than the determined critical ones are presented. The obtained coefficients are presented in Table 2.

Num. scheme	$c_{\mathrm{TVD}}(s,k,r)$	c_{eff}
SSPERK WENO (2,2,3)	0.81	0.41
SSPERK WENO (3,3,4)	0.70	0.23
SSPERK WENO (5,4,5)	1.09	0.22
SDIRK WENO (1,2,3)	0.96	0.96
SDIRK WENO (2,2,3)	1.62	0.81
SDIRK WENO (3,2,3)	3.05	1.02
SDIRK WENO (2,3,4)	1.52	0.76
SDIRK WENO (3,3,4)	2.60	0.87
SDIRK WENO (4,3,4)	2.95	0.74
SDIRK WENO (5,3,4)	3.62	0.72
SDIRK WENO (3,4,5)	1.56	0.52
SDIRK WENO (4,4,5)	1.62	0.41
SDIRK WENO (5,4,5)	2.40	0.48
SDIRK WENO (6,4,5)	3.25	0.54
SDIRK WENO (7,4,5)	3.50	0.50
SDIRK WENO (8,4,5)	3.60	0.45

Table 2. *Test 4.2 – Stability coefficients for different explicit and semi-implicit numerical schemes with finite volume WENO space discretizations*
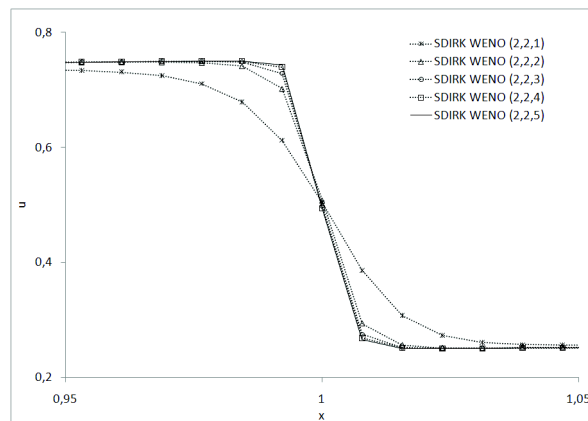

Figure 5. *TEST 4.2 – Comparison of numerical results obtained with semi-implicit WENO schemes with different orders of WENO reconstruction, CFL=1, $t = 2s$*

We have to mention that numerical schemes with the forward Euler time integration and WENO space discretization were quite unstable on this test problem. Therefore, we could not determine the practical SSP coefficient $\sigma_{\mathrm{SSP}}(s,k,r)$ as we did for the linear advection test. Instead, we determine here just stability TVD coefficients $c_{\mathrm{TVD}}(s,k,r)$. The results presented in Table 2 are very similar to those obtained for the linear advection test. Although it seems that these coefficients are mostly larger for the nonlinear case, such a conclusion cannot be made in general. However, our numerical investigations approve that the critical CFL coefficients that were experimentally determined in the linear scalar case can also be used in practical

calculations for the nonlinear scalar case.

Furthermore, we perform the numerical computations by using the semi-implicit WENO schemes with the second order SDIRK time integration with two stages and for different order of WENO space discretization. Comparison of the solutions obtained with the same time step integration method with CFL=1 and for different orders of WENO reconstruction are presented in Figure 5.

4.3. Euler equations

The behaviour of numerical schemes is tested on the one-dimensional Euler system. Euler equations are defined with (1), where the state vector and the flux are equal to

$$\mathbf{u} = \begin{pmatrix} \rho \\ \rho v \\ E \end{pmatrix}, \quad \mathbf{f} = \begin{pmatrix} \rho v \\ \rho v^2 + p \\ v(E + p) \end{pmatrix}. \tag{23}$$

Here ρ, v, E, and p denote the density, velocity, total energy, and pressure, respectively. For the ideal polytropic gas, the equation of state

$$E = \frac{p}{\gamma - 1} + \frac{1}{2}\rho v^2 \tag{24}$$

is valid, with $\gamma = 1.4$. The Jacobian matrix of the system with the corresponding eigenvalues and eigenvectors can be found, for example, in [18, 13].

We analyze numerical schemes on two Riemann problems with known analytical solutions.

4.3.1. Lax test

The Lax problem is defined with the Riemann initial conditions

$$(\rho, v, p) = \begin{cases} (0.445, 0.698, 3.528) \ , \ x \leq 0 \\ (0.5, 0, 0.571) \qquad , \ x > 0. \end{cases} \tag{25}$$

This is a typical test problem for investigating the shock capturing properties of the numerical schemes. We discuss the behaviour and stability properties of the considered finite volume WENO schemes with different SSP time integration methods.

Since the exact solution of a nonlinear system is not necessary TVD (see [13]), a TVD property of the numerical solution should not be a matter of concern. Therefore, the procedure for measuring the practical SSP coefficients performed in the linear scalar case is not applicable any more. Instead, we consider numerical results obtained by using critical CFL coefficients $c_{\text{TVD}}(s, k, r)$ that were determined in Test 4.1.1. In all cases very accurate and stable numerical results are obtained. From the results computed with greater CFL numbers we can conclude that the stability region for this test is even larger than for the considered linear advection test. Thus, similarly as in the case of the Burger's equation, one can conclude that the critical TVD coefficients that were experimentally determined in the linear scalar case can also be used for the nonlinear systems.
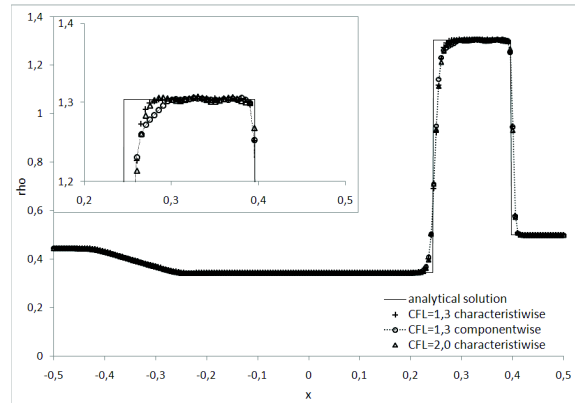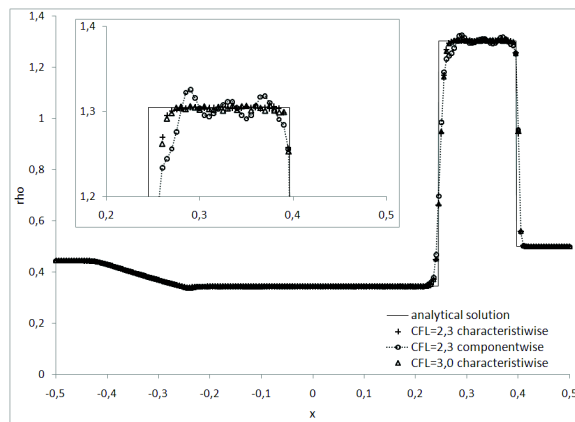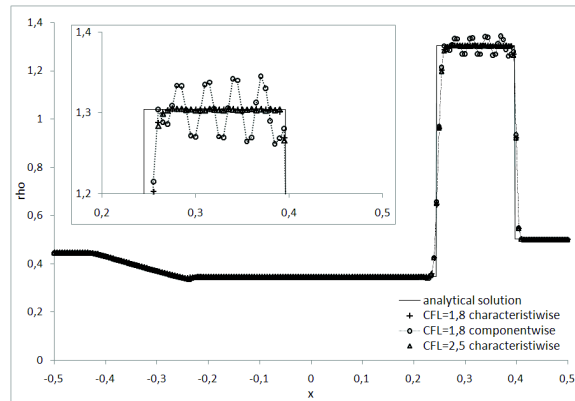
(a) *SDIRK WENO (2,2,3)*

(b) *SDIRK WENO (3,3,4)*

(c) *SDIRK WENO (4,4,5)*

Figure 6. *TEST 4.3.1 – Comparison of numerical results obtained with different reconstruction and different CFL coefficients. Density, $t = 0.16s$*

Num. scheme	$c_{\text{TVD}}(s,k,r)$	Num. scheme	$c_{\text{TVD}}(s,k,r)$
SSPERK WENO (2,2,3)	1.20	SDIRK WENO (4,3,4)	6.80
SSPERK WENO (3,3,4)	1.30	SDIRK WENO (5,3,4)	9.20
SSPERK WENO (5,4,5)	2.40	SDIRK WENO (3,4,5)	3.00
SDIRK WENO (1,2,3)	2.00	SDIRK WENO (4,4,5)	4.20
SDIRK WENO (2,2,3)	3.00	SDIRK WENO (5,4,5)	5.70
SDIRK WENO (3,2,3)	6.00	SDIRK WENO (8,4,5)	11.50
SDIRK WENO (2,3,4)	2.90	SDIRK WENO (7,4,5)	11.00
SDIRK WENO (3,3,4)	4.70		

Table 3. *Test 4.3.2 – Stability coefficients for different semi-implicit numerical schemes with finite volume WENO space discretizations*

Additionally, we compare the results obtained by the componentwise and characteristicwise WENO reconstruction. The results are presented in Figure 6. Numerical oscillations appear when the componentwise approach is used. Such numerical oscillations were also detected for the finite volume and central explicit WENO scheme with componentwise reconstruction (see [14, 1]).

4.3.2. Test with two rarefactions

The considered test is defined with the initial conditions

$$(\rho, v, p) = \begin{cases} (1, -3.1, 1) \;, \; x \leq 0.5 \\ (1, 3.1, 1) \;\;\; , \; x > 0.5 \end{cases} \tag{26}$$
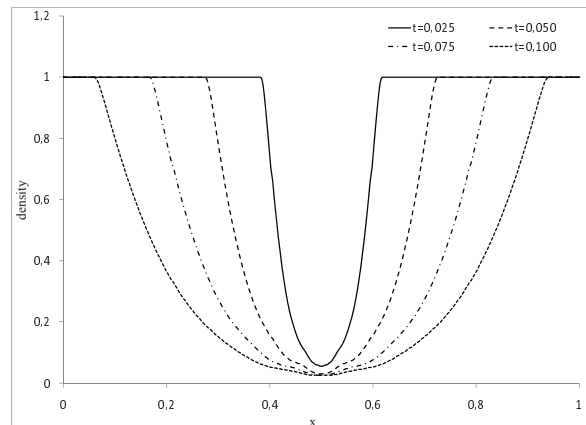

Figure 7. *TEST 4.3.2 – Numerical solution at different time moments obtained with the SSPERK WENO (3,3,4) scheme*

The solution consists of two rarefaction waves and a trivial stationary contact discontinuity, with a very small pressure (near vacuum). This test was also used in [11] for analyzing schemes stability. As stated in the previous test, since the exact solution of a nonlinear system is not TVD in any reasonable sense, we consider now some other form of scheme stability. In this test the numerical scheme is assumed to

be stable if the positivity of density and pressure are preserved. Numerical results at different time moments as an example of the stable scheme behaviour are shown in Figure 7. We evaluated the maximal CFL numbers for which the stated stability criteria are satisfied and present them for different numerical schemes in Table 3. For all considered schemes, the obtained values were greater than the practical CFL coefficient determined in Test 4.1.1.

5. Concluding remarks

In this paper we analyze the behaviour of numerical schemes for hyperbolic conservation laws obtained by combining SSP time integration methods and finite volume WENO space discretization methods. The paper includes a review of the state of the art results about optimal SSP explicit and singly diagonally implicit SSP Runge-Kutta methods. Also, a brief description of the WENO reconstruction procedure and the finite volume WENO discretization is given. Additionally, the semi-implicit WENO scheme obtained by the linearization process of the implicit WENO scheme is presented.

We focus here on practical analysis of SSP coefficients, defined as coefficients for which the stability in total variation seminorm of the first order Euler forward method is maintained for numerical schemes with a higher order temporal discretization but with the same spatial discretization. In this work, the SSP coefficients for the considered finite volume WENO schemes are practically determined on the linear scalar case. From the obtained results, we can conclude that although there exist no theoretical results that finite volume WENO discretization satisfies the TVD property, the coefficients obtained on this linear case are comparable with the theoretically established SSP coefficients valid for TVD numerical schemes. Furthermore, we perform computations on the nonlinear scalar Burgers equation and on Euler equations for gas dynamics. The obtained numerical results show that the schemes perform stable if the experimentally determined CFL coefficients on the linear advection case are used. Based on this numerical study, we can conclude that these coefficients can also be used as the barrier for the stable scheme behaviour on the nonlinear problems.

References

[1] N. Črnjarić–Žic, S. Vuković, L. Sopta, *Balanced finite volume WENO and central WENO schemes for the shallow water and the open channel flow equations*, J. Comput. Phys. **200**(2004), 512–548.

[2] B. Crnković, N. Črnjarić–Žic, L. Kranjčević, *Improvements of semi-implicit schemes for hyperbolic balance laws applied on open channel flow equations*, Comp. Math. with Appl. **58**(2009), 292–309.

[3] L. Ferracina, M. N. Spijker, *Strong stability of singly diagonally implicit Runge-Kutta methods*, Appl. Num. Math. **58**(2008), 1675–1686.

[4] L. Ferracina, M. N. Spijker, *An extension and analysis of the Shu-Osher representation of Runge-Kutta methods*, Math. of Comput. **249**(2005), 201–219.

[5] S. Gottlieb, C.–W. Shu, E. Tadmor, *Strong stability-preserving high-order time discretization methods*, SIAM Review **43**(2001), 89–112.

[6] S. Gottlieb, C.–W. Shu, *Total variation diminishing Runge-Kutta schemes*, Math. Comp. **67**(1998), 73–85.

[7] S. Gottlieb, D. I. Ketcheson, C.-W. Shu, *High order strong stability preserving time discretizations*, J. of Sci. Comp. **38**(2009), 251–289.

[8] S. Gottlieb, J. S. Mullen, S. J. Ruuth, *A fifth order flux implicit WENO method*, J. of Sci. Comp. **27**(2006), 271–287.

[9] A. Harten, B. Engquist, S. Osher, S. Chakravarthy, *Uniformly high order accurate essentially non-oscillatory schemes III*, J. Comput. Phys. **71**(1987), 231–303.

[10] G.–S. Jiang, C.–W. Shu, *Efficient implementation of weighted ENO schemes*, J. Comput. Phys. **126**(1996), 202–228.

[11] D. I. Ketcheson, C. B. Macdonald, S. Gottlieb, *Optimal implicit strong stability preserving Runge-Kutta methods*, Applied Num. Math. **59**(2009), 373–392.

[12] J. F. B. M. Kraajievanger, *Contractivity of Runge-Kutta methods*, BIT **31**(1991), 482–528.

[13] R. J. LeVeque, *Finite Volume Methods for Hyperbolic Problems*, Cambridge University Press, Cambridge, 2002.

[14] J. Qiu, C.–W. Shu, *On the construction, comparison, and local characteristic decomposition for high order central WENO schemes*, J. Comput. Phys. **183**(2002), 187–209.

[15] C.–W. Shu, *Essentially non-oscillatory and weighted essentially non-oscillatory schemes for hyperbolic conservation laws*, in: *Advanced Numerical Approximation of Nonlinear Hyperbolic Equations*, (B. Cockburn, C. Johnson, C.–W. Shu and E. Tadmor, Eds.), Springer-Verlag, Berlin/New York, **1697**(1998), 325–432.

[16] C.–W. Shu, S. Osher, *Efficient implementation of essentially non-oscillatory shock capturing schemes II*, J. Comput. Phys. **83**(1989), 32–78.

[17] R. J. Spiteri, S. J. Ruuth, *A new class of optimal high order strong stability preserving time discretization method*, SIAM J. on Num. Anal. **40**(2002), 469–491.

[18] E. F. Toro, *Riemann Solvers and Numerical Methods in Fluid Dynamics*, Springer, 1999.

[19] H. C. Yee, *Linearised form of implicit TVD schemes for the multidimensional euler and Navier-Stokes equations*, Comput. Math. Appl. **12**(1986), 413–432.

[20] H. C. Yee, *Construction of explicit and implicit symmetric TVD schemes and their applications*, J. Comput. Phys. **68**(1987), 151–179.